Cytoarchitectonically-defined volumes of early extrastriate visual cortex in unmedicated adults with body dysmorphic disorder

Jamie D. Feusner[1,2,3,4,*], **Florian Kurth**[5], **Eileen Luders**[5,6], **Ronald Ly**[4], **Wan-wa Wong**[1,2]

[1] Centre for Addiction and Mental Health, Toronto, Canada

[2] Department of Psychiatry, University of Toronto, Toronto, Canada

[3] Department of Women's and Children's Health, Karolinska Institutet, Stockholm, Sweden

[4] Department of Psychiatry and Biobehavioral Sciences, School of Medicine, University of California Los Angeles, Los Angeles, USA

[5] School of Psychology, University of Auckland, Auckland, New Zealand

[6] Laboratory of Neuro Imaging, School of Medicine, University of Southern California, Los Angeles, USA

Abstract

Background: Individuals with body dysmorphic disorder (BDD) misperceive that they have prominent defects in their appearance, resulting in preoccupations, time-consuming rituals, and distress. Previous neuroimaging studies have found abnormal activation patterns in the extrastriate visual cortex, which may underlie experiences of distorted perception of appearance. Correspondingly, we investigated gray matter volumes in individuals with BDD in the early extrastriate visual cortex using cytoarchitectonically-defined maps that were previously derived from post-mortem brains.

Methods: We analyzed T1-weighted MRI data from 133 unmedicated male and female participants (BDD: n=65; healthy controls: n=68). We used cytoarchitectonically-defined probability maps for the early extrastriate cortex, consisting of areas corresponding to V2, V3d, V3v/VP, V3a, and V4v. Gray matter volumes were compared between groups, supplemented by testing associations with clinical symptoms.

Results: The BDD group exhibited significantly larger gray matter volumes in the left and right early extrastriate cortex. Region-specific follow-up analyses revealed multiple subregions showing larger volumes in BDD, most prominently in left V4v. There were trends for negative associations between gray matter volumes in early extrastriate cortex and BDD symptoms, but not with other comorbid symptoms or duration of illness.

Conclusions: Greater volumes and subvolumes of the early extrastriate visual cortex were evident in those with BDD, which corroborates outcomes of prior studies revealing BDD-specific

*Correspondence should be addressed to: **Jamie Feusner, M.D.**, 250 College St., Toronto, ON M5T 1R8, Canada, jamie.feusner@utoronto.ca.

functional abnormalities in these regions. Enlarged volumes of the extrastriate cortex in BDD might manifest during neurodevelopment, which could predispose individuals to aberrant visual perception and contribute to the core phenotype of distortion of perception for appearance.

1. Introduction

Body dysmorphic disorder (BDD) is characterized by distressing preoccupations with misperceived defects or flaws in one's appearance that are not noticeable or appear slight to others, and repetitive behaviors, typically to check or fix one's appearance (1). BDD has a point prevalence of 1.7%–2.9% in the general population (2–5) and of 13% in psychiatric inpatients (6). The lifetime rate of suicide attempts in BDD is very high, at approximately 25% (7). Despite the prevalence and severity, the underlying neurobiology remains understudied.

A hallmark phenomenological feature of BDD is distorted perception of appearance. The influence of this behavioral phenotype is underscored by the fact that appearance distortions in BDD are often delusional in nature (8). This suggests the possibility that aberrant brain function and structure underpinning disturbed visual information processing may have a prominent role in symptom formation (9–11).

Several neuropsychological and psychophysical studies have revealed abnormalities in visual processing and visuospatial organization, manifesting as deficiencies in global perception and feature integration, accompanied by over-attention to details (12–17). Our previous neuroimaging studies using own face (18), other face (19,20), object stimuli (20,21), and body stimuli (22) point to abnormalities in primary and secondary visual processing systems, particularly when images are filtered to selectively convey configural and holistic information. More specifically, we found evidence of hypoactivation in visual cortical areas including V1, V2, V3V and V4 for viewing own faces, in addition to significant associations between activity in occipital regions and both BDD symptom severity and how aversive participants rated the appearance of their face (18,19). In a joint EEG and fMRI study of visual processing of others' faces and houses, the BDD group demonstrated hypoactivation in V2, V3V, and dorsal visual stream regions (20). These data may reflect in BDD a pathological under-utilization of brain systems dedicated to processing of low levels of detail (global processing). The phenotype may, in turn, explain the increased attention given to miniscule defects and the inability to process these perceptions contextually, i.e., to see them as inconsequential relative to the face or body as a whole, resulting in a perception of a distorted appearance (10). In the aforementioned study (20), we also found hyperactivation for processing of high detail images in BDD in ventral visual stream (temporal fusiform) regions for viewing others' faces. Moreover, the degree of hyperactivation in this region was directly associated with how unattractive BDD participants perceived the face to be. In sum, individuals with BDD exhibit abnormalities

in visual systems involved in global/configural processing as well as local/detail processing, which may contribute to perceptual distortions for one's appearance.

In addition to the above neurocognitive, psychophysical, and functional neuroimaging studies, several studies have examined brain anatomy in BDD compared with healthy controls. Previous studies, albeit with small sample sizes, found reduced regional volumes or thinner cortices (23–25), abnormal brain asymmetries (26), or no differences from controls (27). Effects were evident in the prefrontal cortex (23,24), the caudate (26), and the left middle temporal and left inferior parietal gyri (25). The largely discrepant results across studies could be due to small sample sizes, including both medicated and unmedicated participants, having different gender ratios, and/or having different comorbidity patterns. Interestingly, the largest morphometric study in BDD to date (BDD: n=49; healthy controls: n=44), which included solely unmedicated participants, found a trend for thicker cortices in the BDD group within the left and right extrastriate visual cortex (28).

Given the preliminary evidence of abnormal function and structure in visual cortical regions in BDD, the goal of this analysis was to specifically compare regional volumes (and subvolumes) of the visual cortex between individuals with BDD and healthy controls. To our knowledge, no other study has yet examined BDD-related abnormalities within the early extrastriate visual cortex, possibly due to the challenges of exactly delineating the respective regions. We addressed this challenge by using cytoarchitectonically-defined probabilistic maps of the early extrastriate areas. This state-of-the-art approach provides advantages over traditional region-of-interest approaches by using microscopically defined boundaries based on histology (rather than macroscopic landmarks), as detailed elsewhere (29–33).

The early extrastriate cortex contains the functionally defined areas V2, V3d, V3v/VP, V3A and V4v, which correspond to the anatomically defined cytoarchitectonic areas hOC2, hOC3d, hOC3v, hOC4d, and hOC4v, respectively (34–36). Functionally, these areas are involved in the early processing of the visual input up to stereoscopic, motion, and contour processing in area V3A (hOC3d), as well as contour and color processing in area V4v (hOC4v). As abnormal processing in these areas will affect all further downstream processing and interpretation of the visual input, and considering the spatial locations of abnormalities from the above-described previous functional imaging studies, we focused our analyses on these early areas.

Based on the previous findings of a trend for thicker cortices in a (smaller) sample of individuals with BDD (28), we hypothesized larger gray matter volumes within the left and right early extrastriate cortex in BDD compared with healthy controls. In addition, we examined associations between early extrastriate cortex gray matter volumes and dimensional measures of the BDD-related symptoms of obsessions/compulsions and poor insight. We hypothesized that larger gray matter volumes in the early extrastriate visual cortex would be associated with more severe obsessions/compulsions and lower insight.

2.   Methods

2.1   Study Sample and Image Data

High-resolution T1-weighted images from 67 participants with BDD and 71 healthy
controls, all right-handed and unmedicated, were obtained from two independent previous
studies focusing on brain function. Every BDD participant received a clinical evaluation by
J.D.F., who has clinical expertise in BDD. Individuals who met criteria for BDD on the
BDD Diagnostic Module for DSM-IV (37) and who scored at least 20 on the BDD version
of the Yale–Brown Obsessive–Compulsive Scale (BDD-YBOCS) (38) were eligible. The
Mini International Neuropsychiatric Inventory was used to determine comorbid diagnoses
(39). We excluded participants who were currently taking psychoactive medications or
had taken them within eight weeks of the study, were currently in cognitive-behavioral
therapy, had a lifetime history of neurological disorders, had any current medical disorder
affecting cerebral metabolism, had current substance use disorder, a lifetime history of
bipolar disorder or a psychotic disorder, or had current psychiatric comorbidities aside from
major depressive disorder (MDD), dysthymic disorder, generalized anxiety disorder (GAD),
or social anxiety disorder (SAD). These were allowed because anxiety and depression are
common symptoms in BDD (1), such that excluding these disorders would lead to a non-
representative sample. Notwithstanding, BDD had to be the primary diagnosis. Scores from
the Body Dysmorphic Disorder version of the Yale-Brown Obsessive Compulsive Scale
(BDD-YBOCS), the Brown Assessment of Beliefs Scale (BABS), the Hamilton Anxiety
Scale (HAMA), and the Montgomery-Åsberg Depression Rating Scale (MADRS) were
obtained for all BDD participants, and scores from the HAMA and MADRS were obtained
for the controls.

For the current sample, the imaging data from one participant with BDD and two controls
had ghosting artifacts and were excluded. In addition, one image from a control had severe
motion artifacts, and one BDD participant was missing information on education, resulting
in an exclusion of these participants from further analysis. The final dataset used for analysis
was thus comprised of 65 participants with BDD and 68 control participants (see Table 1
for further sample characterization). Images for 32 BDD and 35 controls were obtained on a
3T Siemens Trio using a 3D T1-weighed MPRAGE sequence with the following parameters:
TR= 1900 ms, TE= 2.26 ms, flip angle = 9°, and a voxel size of $0.98{\times}0.98{\times}1$ mm^3. Images
for a further 33 BDD and 33 controls were acquired on a 3T Siemens Prisma using a 3D
T1-weighed MPRAGE sequence with the following parameters: TR= 2300 ms, TE= 2.27
ms, flip angle = 8°, and a voxel size of $0.8{\times}0.8{\times}0.8$ mm^3. All protocols and procedures were
approved by the institutional review board at UCLA, and participants gave their written and
informed consent.

2.2   Data Processing

The T1-weighted images were processed via the CAT12 toolbox (version 12.6) and SPM12
(r7487), as described elsewhere (29–33). Briefly, the images were tissue was classified
into gray matter, white matter and cerebrospinal fluid using a partial volume estimation
algorithm (40). White matter hyperintensities were masked to prevent their misclassification
as gray matter. The resulting gray matter segments were spatially normalized to the

shooting template within the CAT12 toolbox at a resolution of $1 \times 1 \times 1$ mm^3 using linear transformations and non-linear warping (41). Subsequently, the normalized gray matter segments were modulated to preserve the original voxel-wise gray matter volume (32,42,43). In addition, the total intracranial volume (TIV) was calculated as the sum of the whole-brain tissue volumes of gray matter, white matter, and cerebrospinal fluid to be later included as a covariate in the statistical model.

2.3 Combining Gray Matter Information with Cytoarchitectonic Tissue Probabilities

The cytoarchitectonic probability maps of the subregions of the extrastriate visual cortex – specifically hOC2, hOC3d, hOC3v, hOC4d, and hOC4v, which refer to V2, V3d, V3v/VP, V3a, and V4v, respectively (34–36) – were obtained via the Anatomy Toolbox version 2.2c (44). These areas were mapped on cell body-stained histology sections of ten post-mortem brains using an observer-independent approach based on changes in the cytoarchitecture (45,46), and subsequently converted into region-specific probability maps in MNI single-subject space (34–36). To calculate the region-specific gray matter volumes, the probability maps were spatially normalized to the Shooting template to ensure an accurate correspondence with the normalized modulated gray matter segments (Section 2.2). Subsequently, the normalized probability maps (hOC2, hOC3d, hOC3v, hOC4d, and hOC4v) were multiplied voxel-wise with these normalized modulated gray matter segments. The resulting voxel-wise measures were then summed up and finally multiplied with the voxel volume, revealing the gray matter volume (in mm^3) for each region, as described elsewhere (32). The gray matter volumes for the early extrastriate region, which was the primary region of interest in the current study, were calculated as the sum of the respective areas (Early Extrastriate Cortex = hOC2+hOC3d+hOC3v+hOC4d+hOC4v). Figure 1 shows the location of the early extrastriate cortex color-coded for its local probability, while the color-coded probability maps for the subregions hOC2, hOC3d, hOC3v, hOC4d, and hOC4v are depicted in Figure 3.

2.4 Primary Statistical Analysis

All statistical analyses were conducted in MATLAB (MathWorks, Natick, MA) using a mass-univariate general linear model. The derived volumes for the left and right early extrastriate cortex were used as dependent variables, while group was the independent variable. Age, sex, TIV, scanner, and years of education were treated as variables of no interest[1]. As the residuals for one region were found to be not normally distributed using Lilliefors tests, significance was established using a Monte-Carlo simulation with 10,000 permutations employing the Smith procedure for covariate handling (47,48). As we hypothesized larger gray matter volumes in the BDD group, the group difference was assessed using one-tailed T-tests. All significance levels were corrected for multiple comparisons by controlling the family-wise error rate (47).

In addition, we performed linear regression analyses between the regional gray matter volumes and BDD-YBOCS and BABS scores, separately, within the BDD group.

---

[1]HAMA and MADRS were not included as covariates as they differed significantly between BDD participants and controls and would therefore be collinear with group differences. Instead, associations with gray matter volumes were assessed separately within the BDD group only.

Specifically, the derived volumes for the left and right early extrastriate cortex of the BDD participants were used as dependent variables, while BDD-YBOCS or BABS was the independent variable. Again, age, sex, TIV, scanner, and years of education were treated as variables of no interest. For consistency, significance was again established using a Monte-Carlo simulation with 10,000 permutations employing the Smith procedure for covariate handling (47,48). As we had no specific hypothesis for the direction of the association, two-tailed T-tests were employed. Again, significance levels were corrected for multiple comparisons by controlling the family-wise error rate (47).

2.5 Exploratory Analyses

As a follow-up to our primary hypothesis of BDD effects on the early extrastriate cortex, we investigated whether any effects were particularly pronounced (or restricted) to any of the extrastriate subareas (hOC2, hOC3d, hOC3v, hOC4d, and hOC4v). For these exploratory analyses, we used the same statistical models as for our primary analyses, except gray matter volumes of left and right hOC2, hOC3d, hOC3v, hOC4d, and hOC4v were the dependent variables.

We conducted additional exploratory linear regression analyses of right and left early extrastriate cortex gray matter volumes with HAMA scores, MADRS scores, and illness duration (months), separately, in the BDD group. As two BDD participants had no information on illness duration, associations between gray matter volume and illness duration were investigated using a sample size of n=63. We used the same models and covariates as for the BDD-YBOCS and BABS, as described above.

3. Results

3.1 Study Sample

Participants with BDD presented with moderate to severe OCD symptoms as reflected in the YBOCS scores (range 20 – 44, mean ± standard deviation = 28.9 ± 5.7) and a wide range of insight as reflected in the BABS scores (range 0 – 23, mean ± standard deviation = 14.8 ± 4.1). As further reflected in Table 1, BDD participants had significantly higher levels of anxiety (p < 0.001) and depression (p < 0.001) compared to controls, as measured using the HAMA and MADRS scales. No significant group differences were observed in age, sex, education, TIV, or scanner.

3.2 Early Extrastriate Gray Matter Volume

As shown in Figure 1, the BDD group had significantly larger gray matter volumes in the early extrastriate visual cortex in both hemispheres. The effects were similar in both hemispheres, with t=2.120, Cohen's d=0.378, and p=0.033 (corrected) on the left, and t=2.109, Cohen's d=0.376, and p=0.033 (corrected) on the right.

3.3 Associations between Early Extrastriate Gray Matter and Clinical Symptoms

Plots for the association between early extrastriate gray matter volumes and obsession/compulsion symptoms (BDD-YBOCS scores) as well as insight (BABS scores) are shown in Figure 2. Relationships between volumes and BDD-YBOCS scores did not survive

corrections for multiple comparisons. Uncorrected, there was a negative association between BDD-YBOCS and left early extrastriate gray matter (r=−0.259, $p_{uncorrected}$ = 0.046). There were no significant associations with BABS at a corrected or uncorrected level.

Exploratory analyses showed no significant associations between left or right early extrastriate gray matter volumes and anxiety (HAMA scores), depression (MADRS scores) (Table S1), or illness duration (Table S2), at a corrected or uncorrected level.

3.4 Exploratory Analyses of Regional Gray Matter Volume

As shown in Figure 3 and Table 3, the BDD group had significantly larger gray matter volumes in left hOC4v (t=0.467, Cohen's d=0.440, p=0.040, corrected). When not correcting for multiple comparisons for this exploratory analysis, further effects were observed in right hOC2 (t=1.829, Cohen's d=0.326, $p_{uncorrected}$=0.037), left hOC3d (t=1.900, Cohen's d=0.339, $p_{uncorrected}$=0.033), right hOC3d (t=1.977, Cohen's d=0.352, $p_{uncorrected}$=0.025), left hOC3v (t=2.157, Cohen's d=0.384, $p_{uncorrected}$=0.016), right hOC4d (t=1.710, Cohen's d=0.305, $p_{uncorrected}$=0.044), as well as right hOC4v (t=2.013, Cohen's d=0.359, $p_{uncorrected}$=0.021).

3.5 Exploratory Associations between Regional Gray Matter and Clinical Symptoms

There were no significant associations between regional gray matter volumes and BDD-YBOCS, BABS, HAMA, or MADRS that survived correction for multiple comparisons (Table S3). Uncorrected, negative associations were observed between BDD-YBOCS and left hOC2 (r=−0.336, $p_{uncorrected}$ = 0.012), right hOC3d (r=−0.295, $p_{uncorrected}$ = 0.023), and right hOC4d (r=−0.299, $p_{uncorrected}$ = 0.023). Plots for the association between regional gray matter and BDD-YBOCS and BABS are shown in Supplementary Figure 1. There were no significant associations between regional gray matter volumes and illness duration, either corrected or uncorrected (Table S4).

4. Discussion

This is the largest morphometric study in BDD to date and the first to examine cytoarchitectonic-defined brain volumes in BDD. We performed a focused volumetric analysis of early extrastriate visual cortical regions given the prior evidence in BDD of functional abnormalities in these regions for symptom- and non-symptom-related visual stimuli. As hypothesized, results demonstrated significantly larger volumes and subvolumes in BDD compared with healthy controls in the early extrastriate cortex as well as negative associations between volumes and BDD symptom severity.

The regions of increased gray matter volume in early extrastriate visual cortex in individuals with BDD overlap with regions where we previously detected reduced activation compared with controls when viewing relevant symptom-related visual stimuli of faces (18–20) as well as non-symptom related stimuli of houses (20). Specifically, we previously found hypoactivation in right and left V2 (and left V1) for viewing others' faces in one study (19) and hypoactivation in left V2 and left V4 when viewing others' and own faces in a second study (18). In addition, we observed hypoactivity for house viewing in right V2, which was associated with the N170 event-related potential component (20) as well as a negative

associations between BDD-YBOCS scores and activation for viewing houses in right V2 (21). Further, hypoactivity was also evident in BDD in more dorsal regions of the occipital and parietal dorsal visual stream when viewing face and house stimuli (20) as well as body stimuli (22).

These results raise the question of why there are larger early extrastriate visual cortical volumes in regions previously found to demonstrate hypoactivity, and if and how this might relate to the core BDD symptom of distorted perception of one's appearance. Theoretically, a larger gray matter volume could point to higher numbers of neurons, synapses, and/or glia cells. This might arise during neurodevelopment due to insufficient synaptic pruning, such as has been theorized for neurodevelopmental disorders including autism spectrum disorder and epilepsy (49). During normal visual neurodevelopment there is a gradual shift in predominantly local perceptual strategies to more global strategies, which occurs from early to later childhood (50) and may continue into adolescence (51–53). Occipital gray matter also decreases linearly in normal development from childhood through adolescence (54). In support of the assumption that BDD occurs as an abnormality of neurodevelopment, the timeframe would correspond to the typical onset of BDD, which is in late childhood or early adolescence (55). Functionally, aberrant visual cortical development and insufficient pruning in individuals who later develop BDD could impact mechanisms related to switching from global to local visual processing strategies. This might manifest as a reduced ability to integrate visual details into a more global context, in accordance with proposed models of the neurobiology of BDD involving imbalances in global vs. local processing (10,56,57). As a result, small details might be experienced as prominent and out of proportion, and thereby as "flawed" and unattractive. The subvolume that showed the largest effect size difference between groups, area hOC4v, corresponding to area V4v, has been classically described as involved in contour and color processing (36). In addition, enhanced functional connectivity between V1 and V4v has been demonstrated to be related to active searching for a target object in a scene, whether memory-based or during free viewing (58); the success of this function might be dependent on detecting characteristics such as color, texture, and simple geometric shape (59).

Alternatively, BDD-related obsessive preoccupation with one's appearance along with symptomatic behaviors (e.g., scrutiny of appearance in mirrors and reflective surfaces and concomitant focused visual attention) could also modify early extrastriate cortical architecture and, as such, result in larger regional volumes. However, the lack of significant association between regional volumes and illness duration might currently argue against this possibility. The mechanisms behind either primary neurodevelopmental abnormalities and/or neuroplastic changes that occur over time, and their relationships to aberrant visual perception or other phenotypes involved in BDD, remain to be directly investigated in future studies.

The results of the current study are largely consistent with the outcomes of our previous whole-brain morphometric study, which investigated point-wise cortical thickness and voxel-wise gray matter (28) in an overlapping sample[2]. More specifically, in our earlier study, the cortex was thicker (albeit not statistically significant) in BDD within the lateral occipital cortex, pericalcarine cortex, lingual cortex, and cuneus. In contrast, two other

studies (both with n=20 vs. n=20) found significantly reduced volumes in BDD in the left occipital lobe and in left/right prefrontal, parietal, temporal, and cerebellar cortices (24) as well as in the left inferior parietal and left middle temporal cortices (25). However, unlike the current sample, all but two of the participants in these two studies were medicated. Since medication has been shown to affect regional brain morphology in psychiatric disorders (60), these findings should be interpreted with caution. Overall, much remains to be investigated regarding brain morphology in BDD, as the field is relatively young in comparison with other psychiatric and neuropsychiatric disorders.

There are several limitations of the current study to consider. We did not perform psychophysical testing or other visual experiments to explore direct associations between cortical volumes and visual perception. Further, given that this was a cross-sectional analysis, the causes of abnormal visual cortical morphology cannot be determined.

In conclusion, this study demonstrates that individuals with BDD exhibit larger volumes and subvolumes of the early extrastriate visual cortex. These structural aberrations are in line with region-specific functional abnormalities from multiple previous studies. This neurobiological phenotype, perhaps a consequence of deviant neurodevelopmental events, might predispose individuals to aberrant visual perception and contribute to the core phenotype of distortion of perception for appearance.

Supplementary Material

Refer to Web version on PubMed Central for supplementary material.

Acknowledgements

References

1. American Psychiatric Association (2013): Diagnostic and Statistical Manual of Mental Disorders (DSM-5®). American Psychiatric Pub.

2. Rief W, Buhlmann U, Wilhelm S, Borkenhagen A, Brähler E (2006): The prevalence of body dysmorphic disorder: a population-based survey. Psychol Med 36: 877–885. [PubMed: 16515733]

3. Buhlmann U, Glaesmer H, Mewes R, Fama JM, Wilhelm S, Brähler E, Rief W (2010): Updates on the prevalence of body dysmorphic disorder: a population-based survey. Psychiatry Res 178: 171–175. [PubMed: 20452057]

4. Koran LM, Abujaoude E, Large MD, Serpe RT (2008): The prevalence of body dysmorphic disorder in the United States adult population. CNS Spectr 13: 316–322. [PubMed: 18408651]

5. Schieber K, Kollei I, de Zwaan M, Martin A (2015): Classification of body dysmorphic disorder - what is the advantage of the new DSM-5 criteria? J Psychosom Res 78: 223–227. [PubMed: 25595027]

6. Mufaddel A, Osman OT, Almugaddam F, Jafferany M (2013): A review of body dysmorphic disorder and its presentation in different clinical settings. Prim Care Companion CNS Disord 15. 10.4088/PCC.12r01464

2Data from 42 BDD and 48 healthy controls were unique to the current study; data from 26 BDD and 21 healthy controls were unique to the earlier study; and data from 23 BDD participants and 23 healthy controls overlapped between the two studies.

7. Phillips KA, Menard W (2006): Suicidality in body dysmorphic disorder: a prospective study. Am J Psychiatry 163: 1280–1282. [PubMed: 16816236]

8. Phillips KA, Hart AS, Simpson HB, Stein DJ (2014): Delusional versus nondelusional body dysmorphic disorder: recommendations for DSM-5. CNS Spectr 19: 10–20. [PubMed: 23659348]

9. Beilharz F, Castle DJ, Grace S, Rossell SL (2017): A systematic review of visual processing and associated treatments in body dysmorphic disorder. Acta Psychiatr Scand 136: 16–36. [PubMed: 28190269]

10. Li W, Arienzo D, Feusner JD (2013): Body Dysmorphic Disorder: Neurobiological Features and an Updated Model. Z Klin Psychol Psychother 42: 184–191.

11. Madsen SK, Bohon C, Feusner JD (2013): Visual processing in anorexia nervosa and body dysmorphic disorder: similarities, differences, and future research directions. J Psychiatr Res 47: 1483–1491. [PubMed: 23810196]

12. Deckersbach T, Savage CR, Phillips KA, Wilhelm S, Buhlmann U, Rauch SL, et al. (2000): Characteristics of memory dysfunction in body dysmorphic disorder. J Int Neuropsychol Soc 6: 673–681. [PubMed: 11011514]

13. Feusner JD, Moller H, Altstein L, Sugar C, Bookheimer S, Yoon J, Hembacher E (2010): Inverted face processing in body dysmorphic disorder. J Psychiatr Res 44: 1088–1094. [PubMed: 20434170]

14. Jefferies K, Laws KR, Fineberg NA (2012): Superior face recognition in Body Dysmorphic Disorder. J Obsessive Compuls Relat Disord 1: 175–179.

15. Stangier U, Adam-Schwebe S, Müller T, Wolter M (2008): Discrimination of facial appearance stimuli in body dysmorphic disorder. J Abnorm Psychol 117: 435–443. [PubMed: 18489220]

16. Mundy EM, Sadusky A (2014): Abnormalities in visual processing amongst students with body image concerns. Adv Cogn Psychol 10: 39–48. [PubMed: 25157299]

17. Dhir S, Ryan HS, McKay EL, Mundy ME (2018): Parameters of visual processing abnormalities in adults with body image concerns. PLoS One 13: e0207585. [PubMed: 30475860]

18. Feusner JD, Moody T, Hembacher E, Townsend J, McKinley M, Moller H, Bookheimer S (2010): Abnormalities of visual processing and frontostriatal systems in body dysmorphic disorder. Arch Gen Psychiatry 67: 197–205. [PubMed: 20124119]

19. Feusner JD, Townsend J, Bystritsky A, Bookheimer S (2007): Visual information processing of faces in body dysmorphic disorder. Arch Gen Psychiatry 64: 1417–1425. [PubMed: 18056550]

20. Li W, Lai TM, Bohon C, Loo SK, McCurdy D, Strober M, et al. (2015): Anorexia nervosa and body dysmorphic disorder are associated with abnormalities in processing visual information. Psychol Med 45: 2111–2122. [PubMed: 25652023]

21. Feusner JD, Hembacher E, Moller H, Moody TD (2011): Abnormalities of object visual processing in body dysmorphic disorder. Psychol Med 41: 2385–2397. [PubMed: 21557897]

22. Moody TD, Morfini F, Cheng G, Sheen CL, Kerr WT, Strober M, Feusner JD (2020): Brain activation and connectivity in anorexia nervosa and body dysmorphic disorder when viewing bodies: relationships to clinical symptoms and perception of appearance. Brain Imaging Behav. 10.1007/s11682-020-00323-5

23. Atmaca M, Bingol I, Aydin A, Yildirim H, Okur I, Yildirim MA, et al. (2010): Brain morphology of patients with body dysmorphic disorder. J Affect Disord 123: 258–263. [PubMed: 19846221]

24. Buchanan B, Rossell S, Maller JJ, Toh WL, Brennan S, Castle D (2014): Regional brain volumes in body dysmorphic disorder compared to controls. Aust N Z J Psychiatry 48: 654–662. [PubMed: 24497623]

25. Grace SA, Buchanan BG, Maller JJ, Toh WL, Castle DJ, Rossell SL (2017): Reduced cortical thickness in body dysmorphic disorder. Psychiatry Res Neuroimaging 259: 25–28. [PubMed: 27918913]

26. Rauch SL, Phillips KA, Segal E, Makris N, Shin LM, Whalen PJ, et al. (2003): A preliminary morphometric magnetic resonance imaging study of regional brain volumes in body dysmorphic disorder. Psychiatry Research: Neuroimaging 122: 13–19.

27. Feusner JD, Townsend J, Bystritsky A, McKinley M, Moller H, Bookheimer S (2009): Regional brain volumes and symptom severity in body dysmorphic disorder. Psychiatry Res 172: 161–167. [PubMed: 19328661]

28. Madsen SK, Zai A, Pirnia T, Arienzo D, Zhan L, Moody TD, et al. (2015): Cortical thickness and brain volumetric analysis in body dysmorphic disorder. Psychiatry Res 232: 115–122. [PubMed: 25797401]

29. Kurth F, Cherbuin N, Luders E (2015): Reduced age-related degeneration of the hippocampal subiculum in long-term meditators. Psychiatry Res 232: 214–218. [PubMed: 25907419]

30. Kurth F, Cherbuin N, Luders E (2017): The impact of aging on subregions of the hippocampal complex in healthy adults. Neuroimage 163: 296–300. [PubMed: 28917699]

31. Kurth F, Jancke L, Luders E (2017): Sexual dimorphism of Broca's region: More gray matter in female brains in Brodmann areas 44 and 45. J Neurosci Res 95: 626–632. [PubMed: 27870461]

32. Kurth F, Jancke L, Luders E (2018): Integrating cytoarchitectonic probabilities with MRI-based signal intensities to calculate regional volumes of interest. Neuromethods. New York, NY: Springer New York, pp 121–129.

33. Luders E, Kurth F, Toga AW, Narr KL, Gaser C (2013): Meditation effects within the hippocampal complex revealed by voxel-based morphometry and cytoarchitectonic probabilistic mapping. Front Psychol 4: 398. [PubMed: 23847572]

34. Amunts K, Malikovic A, Mohlberg H, Schormann T, Zilles K (2000): Brodmann's areas 17 and 18 brought into stereotaxic space-where and how variable? Neuroimage 11: 66–84. [PubMed: 10686118]

35. Kujovic M, Zilles K, Malikovic A, Schleicher A, Mohlberg H, Rottschy C, et al. (2013): Cytoarchitectonic mapping of the human dorsal extrastriate cortex. Brain Struct Funct 218: 157–172. [PubMed: 22354469]

36. Rottschy C, Eickhoff SB, Schleicher A, Mohlberg H, Kujovic M, Zilles K, Amunts K (2007): Ventral visual cortex in humans: cytoarchitectonic mapping of two extrastriate areas. Hum Brain Mapp 28: 1045–1059. [PubMed: 17266106]

37. Phillips KA, Atala KD, Pope HG Jr. (1995): Diagnostic instruments for body dysmorphic disorder. presented at the American Psychiatric Association 148th Annual Meeting.

38. Phillips KA, Hollander E, Rasmussen SA, Aronowitz BR, DeCaria C, Goodman WK (1997): A severity rating scale for body dysmorphic disorder: development, reliability, and validity of a modified version of the Yale-Brown Obsessive Compulsive Scale. Psychopharmacol Bull 33: 17–22. [PubMed: 9133747]

39. Lecrubier Y, Sheehan D, Hergueta T, Weiller E (1998): The mini international neuropsychiatric interview. European Psychiatry, vol. 13. p 198s.

40. Tohka J, Zijdenbos A, Evans A (2004): Fast and robust parameter estimation for statistical partial volume models in brain MRI. Neuroimage 23: 84–97. [PubMed: 15325355]

41. Ashburner J, Friston KJ (2011): Diffeomorphic registration using geodesic shooting and Gauss–Newton optimisation. Neuroimage 55: 954–967. [PubMed: 21216294]

42. Ashburner J, Friston KJ (2000): Voxel-based morphometry--the methods. Neuroimage 11: 805–821. [PubMed: 10860804]

43. Good CD, Johnsrude IS, Ashburner J, Henson RN, Friston KJ, Frackowiak RS (2001): A voxel-based morphometric study of ageing in 465 normal adult human brains. Neuroimage 14: 21–36. [PubMed: 11525331]

44. Eickhoff SB, Stephan KE, Mohlberg H, Grefkes C, Fink GR, Amunts K, Zilles K (2005): A new SPM toolbox for combining probabilistic cytoarchitectonic maps and functional imaging data. Neuroimage 25: 1325–1335. [PubMed: 15850749]

45. Schleicher A, Amunts K, Geyer S, Kowalski T, Schormann T, Palomero-Gallagher N, Zilles K (2000): A stereological approach to human cortical architecture: identification and delineation of cortical areas. J Chem Neuroanat 20: 31–47. [PubMed: 11074342]

46. Schleicher A, Palomero-Gallagher N, Morosan P, Eickhoff SB, Kowalski T, de Vos K, et al. (2005): Quantitative architectural analysis: a new approach to cortical mapping. Anat Embryol (Berl) 210: 373–386. [PubMed: 16249867]

47. Friston K, Ashburner J, Kiebel S, Nichols TE, Penny WD (n.d.): Non-parametric procedures. Statistical Parametric Mapping: The Analysis of Functional Brain Images.

48. Winkler AM, Ridgway GR, Webster MA, Smith SM, Nichols TE (2014): Permutation inference for the general linear model. Neuroimage 92: 381–97. [PubMed: 24530839]

49. Neniskyte U, Gross CT (2017): Errant gardeners: glial-cell-dependent synaptic pruning and neurodevelopmental disorders. Nat Rev Neurosci 18: 658–670. [PubMed: 28931944]

50. Nayar K, Franchak J, Adolph K, Kiorpes L (2015): From local to global processing: The development of illusory contour perception. J Exp Child Psychol 131: 38–55. [PubMed: 25514785]

51. Scherf KS, Behrmann M, Kimchi R, Luna B (2009): Emergence of global shape processing continues through adolescence. Child Dev 80: 162–177. [PubMed: 19236399]

52. Hadad B-S, Maurer D, Lewis TL (2010): The development of contour interpolation: evidence from subjective contours. J Exp Child Psychol 106: 163–176. [PubMed: 20227089]

53. Kimchi R, Hadad B, Behrmann M, Palmer SE (2005): Microgenesis and ontogenesis of perceptual organization: evidence from global and local processing of hierarchical patterns. Psychol Sci 16: 282–290. [PubMed: 15828975]

54. Brain Development Cooperative Group (2012): Total and regional brain volumes in a population-based normative sample from 4 to 18 years: The NIH MRI study of normal brain development. Cereb Cortex 22: 1–12. [PubMed: 21613470]

55. Gunstad J, Phillips KA (2003): Axis I comorbidity in body dysmorphic disorder. Compr Psychiatry 44: 270–276. [PubMed: 12923704]

56. Grace SA, Labuschagne I, Kaplan RA, Rossell SL (2017): The neurobiology of body dysmorphic disorder: A systematic review and theoretical model. Neurosci Biobehav Rev 83: 83–96. [PubMed: 29017915]

57. Feusner JD, Neziroglu F, Wilhelm S, Mancusi L, Bohon C (2010): What Causes BDD: Research Findings and a Proposed Model. Psychiatr Ann 40: 349–355. [PubMed: 24347738]

58. Jo H-G, Ito J, Schulte Holthausen B, Baumann C, Grün S, Habel U, Kellermann T (2019): Task-dependent functional organizations of the visual ventral stream. Sci Rep 9: 9316. [PubMed: 31249350]

59. Roe AW, Chelazzi L, Connor CE, Conway BR, Fujita I, Gallant JL, et al. (2012): Toward a unified theory of visual area V4. Neuron 74: 12–29. [PubMed: 22500626]

60. Boedhoe PSW, Schmaal L, Abe Y, Alonso P, Ameis SH, Anticevic A, et al. (2018): Cortical Abnormalities Associated With Pediatric and Adult Obsessive-Compulsive Disorder: Findings From the ENIGMA Obsessive-Compulsive Disorder Working Group. Am J Psychiatry 175: 453–462. [PubMed: 29377733]
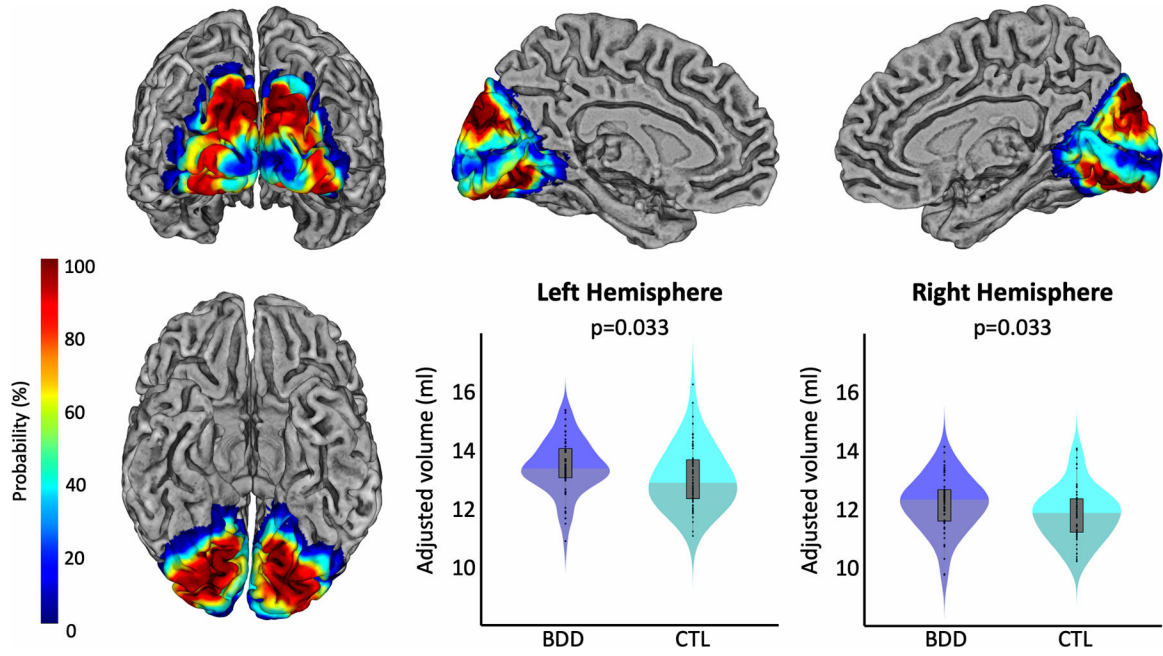
Figure 1.

Group differences in the gray matter volume of the early extrastriate cortex. The renderings depict the local probability of each voxel to belong to any of the regions of interest. The left column shows a view of the ROI from occipital (top) and inferior (bottom). The top row further shows views of the ROI of the left medial (middle) and right medial hemisphere (right). The violin plots present the respective gray matter volumes within this region in blue for participants with BDD and in cyan for controls. Left hemispheric volumes are shown in the middle and right hemispheric volumes on the right of the bottom row. All gray matter volumes are adjusted for age, sex, total intracranial volume, years of education, and scanner. Significance values are corrected for multiple comparisons.
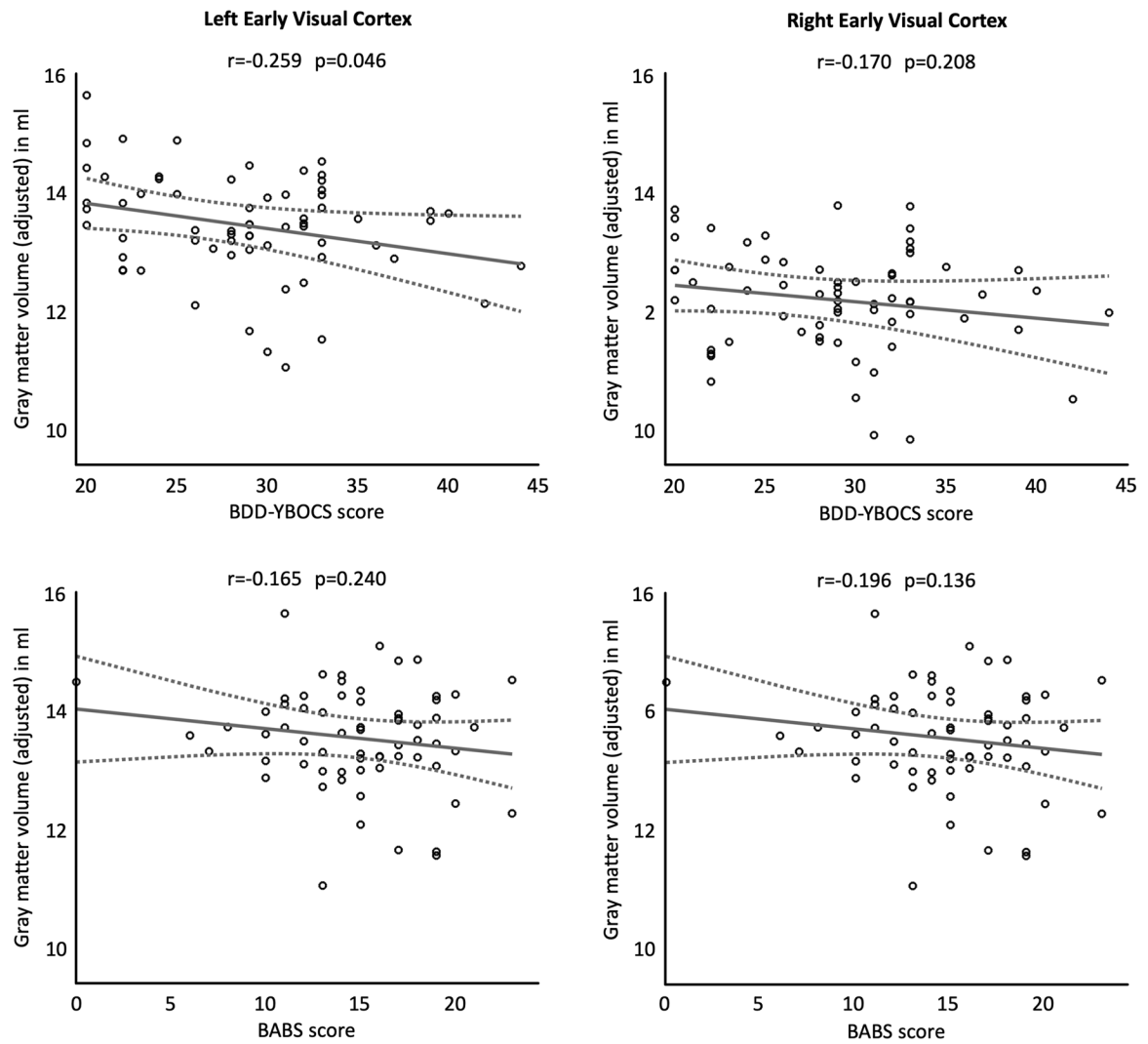
Figure 2.
Associations between gray matter volume of the early extrastriate cortex and obsessions/compulsions (BDD-YBOCS score, top row) and insight (BABS score, bottom row). The left column depicts left-hemispheric and the right column right-hemispheric measures. The least-squares regression lines are plotted as solid lines, the 95% confidence intervals are shown as dashed lines. All gray matter volumes are adjusted for age, sex, total intracranial volume, years of education, and scanner. The given significance values are uncorrected.
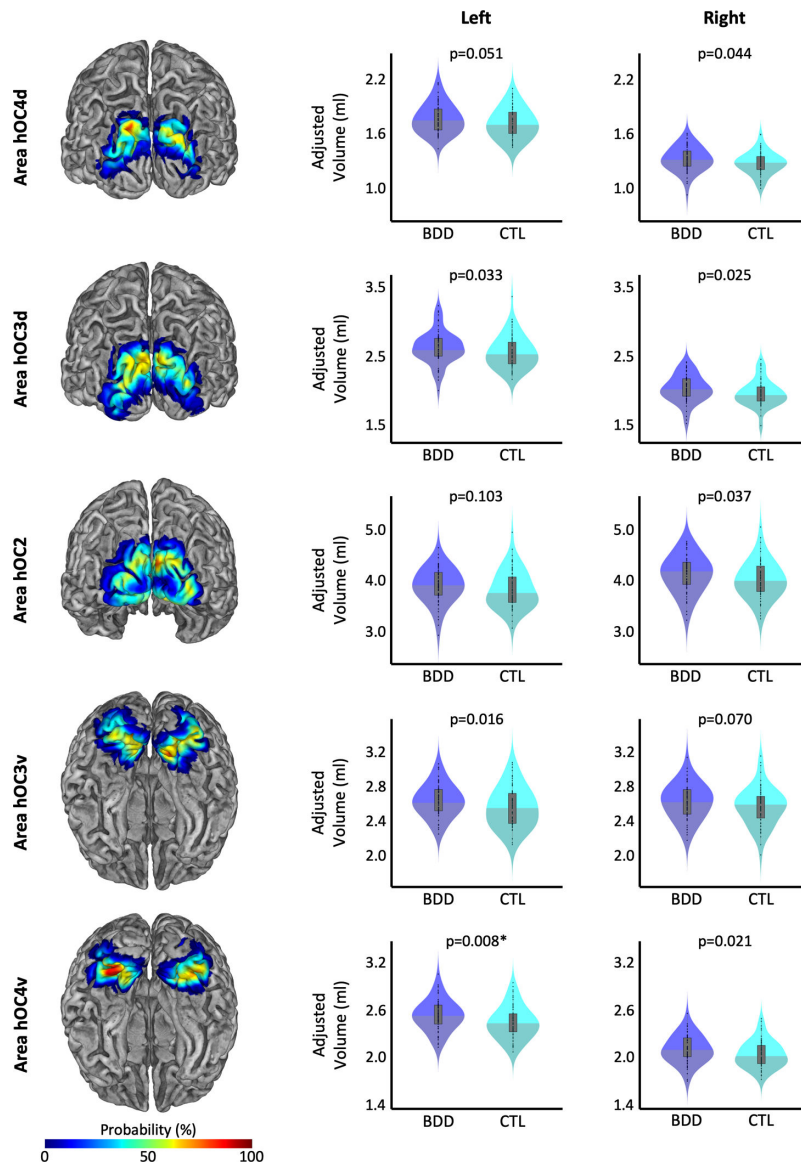
Figure 3.
Group differences in regional gray matter volumes. Probabilistic maps of the cytoarchitectonic regions of the early extrastriate cortex, which served as the regions of interest, are depicted on the left with a posterior view (top three) or inferior view (bottom two). The respective violin plots of the gray matter volumes in participants with BDD (shown in blue) and controls (shown in cyan) are depicted in the middle for the left hemisphere and the right for the right hemisphere. All gray matter volumes are adjusted for age, sex, total intracranial volume, years of education, and scanner. The asterisk indicates the group difference that survived correction for multiple comparisons.

Table 1.

Sample characteristics

	BDD	CTL	
N	65	68	
Sex	55 F / 10 M	53 F / 15 M	p = 0.379[a]
Age (years)	23.5 ± 6.1	22.6 ± 6.6	p = 0.414[b]
TIV (ml)	1416.2 ± 105.2	1414.3 ± 154.8	p = 0.934[b]
Education (years)	14.4 ± 2.7	13.7 ± 2.3	p = 0.934[b]
Scanner	33 Prisma / 32 Trio	33 Prisma / 35 Trio	p = 0.863[a]
HAMA	11.1 ± 7.2	2.3 ± 2.0	p < 0.001[c]
MADRS	15.4 ± 9.0	1.1 ± 1.6	p < 0.001[c]
Illness Duration (months)[d]	111 ± 88	-	-
Psychiatric Comorbidities [e]			
Major depressive episode	18	-	-
Persistent depressive disorder (dysthymia)	7	-	-
Panic disorder with agoraphobia	3	-	-
Agoraphobia without history of panic disorder	3	-	-
Social phobia	8	-	-
PTSD	2	-	-
Generalized anxiety disorder	15	-	-
Obsessive compulsive disorder	1	-	-
No DSM comorbid disorder	27	-	-

[a]Calculated using Fisher's exact test

[b]Calculated using a two-sample T-test

[c]Calculated using a two-sample T-test with unequal variance

[d]Data for two patients is missing

[e]Some patients may have more than one comorbidity